

Phylogeography of the Rice Spittle Bug (*Callitettix versicolor*) Implies Two Long-Term Mountain Barriers in South China

Han Yang¹, Chung-Ping Lin², and Ai-Ping Liang^{1*}

¹Key Laboratory of Zoological Systematics and Evolution, Institute of Zoology, Chinese Academy of Sciences, Beijing, China

²Department of Life Science, National Taiwan Normal University, Taipei, Taiwan

South China is a region of remarkable topographic complexity. However, the impact of climate fluctuations in the Pleistocene on the local fauna and especially insects has not been extensively studied. We integrated mitochondrial DNA (mtDNA) and microsatellite data of the rice spittle bug, *Callitettix versicolor*, to determine the genetic structure, potential biogeographic barriers, and historical demography of this species. The mtDNA data revealed two distinct lineages (Western and Eastern) congruent with the geographically separated western and eastern sub-regions of the Hengduan Mountains. The Eastern lineage was subdivided into two sub-lineages, E1 and E2, congruent with the geographically separated northern and southern sub-regions of the Dabie Mountains. E2 was further subdivided into two sub-groups, E2-1 and E2-2, with a hybrid zone (Guizhou and Hunan Provinces) in which their areas were contiguous. The genetic structures constructed using mtDNA were corroborated by four clusters (G1–G4) of microsatellite data. The populations of each cluster were nearly consistent with a sub-lineage of the mtDNA gene tree (G1–G4 corresponded to the Western, E1, E2-2 and E2-1 lineages, respectively). The divergence time estimated between the Western and Eastern lineages was 1.17 (0.50–2.37) to 0.89 (0.39–1.78) Mya, indicating that the lineages diversified on both geographic and temporal scales. The historical demography of the Eastern lineage showed continuous population growth after the Last Interglacial (LIG) and a stable population during the Last Glacial Maximum (LGM) period. However, the Western lineage remained largely unchanged during the LIG and LGM periods. This suggests that the historical demography of *C. versicolor* is probably related not only to the paleoclimate of South China, but also to the geological restriction and specific habitat preferences of species.

Key words: *Callitettix versicolor*, phylogenetic tree, phylogeography, historical demography, ecological niche modeling

INTRODUCTION

Climatic fluctuations during the Pleistocene shaped the patterns of genetic diversity in many extant temperate species (Avice et al., 1998; Hewitt, 1996). For example, during the Pleistocene glaciations, Europe and most regions of North America were covered with ice sheets (Hewitt, 1996, 2000). As global cooling progressed during the Last Glacial Maximum (LGM, 0.015–0.025 Mya), temperate species retracted into smaller refugial areas. They subsequently expanded out of the refugia as temperatures increased during the post-LGM period (Hewitt, 1996; Runck and Cook, 2005). However, several recent studies of East Asian species have revealed a different expansion period from that of Europe and North America, with demographic expansion occurring before the LGM (Li et al., 2009; Huang and Lin, 2010; Huang et al., 2010b; Qu et al., 2011; Zhao et al., 2012). This pre-LGM demographic expansion may have

been associated with a wetter climate and the absence of large glaciers during the ice ages in the lower latitudes of East Asia (Pinot et al., 1999; Shi and Yao, 2002; Zhang et al., 2006).

South China was a globally important Pleistocene refugium for species that evolved prior to the late Tertiary and Quaternary glaciations (Patriat and Achaté, 1984). The uplift of the Tibetan Plateau approximately three million years ago caused a gradually descending topography to develop from west to east in South China. In southwest China, mountains form a series of parallel alpine ranges rising to altitudes over 5000 m, the differences in altitude between valleys and mountaintops often exceeding 2000 m. The complex topography of southwest China led to long-term geographic isolation and resulted in dramatic ecological stratification of many endemic taxa (Li, 1989; Zhang et al., 2006; Huang et al., 2010a; Qu et al., 2011). Compared with southwest China (Tibetan Plateau), a biodiversity hot spot, much less attention has been given to the biogeography of southeast China, where there is a mosaic of mountains lower than 2000 m together with complicated river systems (Maddison and McMahon, 2000; Masta, 2000; Knowles, 2001). The topographical simplicity and a milder Pleistocene

* Corresponding author. Tel. : +86-10-64807226;
Fax : +86-10-64807099;
E-mail: liangap@ioz.ac.cn

Supplemental material for this article is available online.
doi:10.2108/zs160042

climate could have mitigated demographic stresses for species in this area (Hewitt, 2000, 2004). However, the general effects of the Pleistocene ice ages on the genetic structures and historical demography of organisms inhabiting this lower altitudinal part of China remain obscure.

In the present study, we investigated the impact of historical climate fluctuations on the diversification of species in South China using the rice spittle bug, *Callitettix versicolor* (Hemiptera: Cercopidae), as exemplar. This insect prefers warm and humid habitats and breeds in paddy fields, ditches and ponds below an altitude of 1200 m. It has limited dispersal on account of its poor flying ability (Chen and Liang, 2012). We used three mitochondrial genes and 11 microsatellite loci to reconstruct the phylogeography and demographic history of *C. versicolor*. The specific aims were: (1) to determine the genetic structure and identify potential biogeographic barriers for *C. versicolor*; (2) to test whether the historical demography of *C. versicolor* was consistent with the prediction derived from pre-LGM demographic expansion.

MATERIALS AND METHODS

Ethics statement

The field and laboratory studies did not involve endangered or protected species. *Callitettix versicolor* is considered a common pest in China and is therefore not included in the "List of Protected Animals in China", and no specific permits were required to collect

insect specimens from farmlands.

Sample collection and laboratory methods

A total of 442 individuals of *C. versicolor* were collected from 24 localities between May and July of 2014 (Table 1, Fig. 1). No specimens were found at high altitudes west of the Tibetan Plateau. The legs of the specimens were dissected and used for genomic DNA extractions with a DNeasy Tissue kit (Qiagen, Hilden, Germany) following the manufacturer's instructions.

Fragments of three mitochondrial genes (cytochrome c oxidase subunit I, *COI*; cytochrome b, *Cytb*; and NADH dehydrogenase subunit 5, *ND5*) were amplified by polymerase chain reactions (PCR) using our newly-designed primer pairs modified from Simon et al. (2006) (Supplementary Table S1). The PCR reactions involved a total volume of 25 μ l, composed of 12.5 μ l dNTP Mixture (Tiangen, Beijing, China), 1 μ l of 10 mM of each primer, 9.5 μ l of deionized water (Tiangen, Beijing, China) and 1 μ l of extracted DNA (80 to 300 ng/ μ l). The PCR conditions were as follows: denaturation at 94°C for 4 min; followed by 40 cycles at 94°C for 1 min, annealing temperature (48°C for *COI* and *Cytb*, 56°C for *ND5*) for 50 s, and 72°C for 40 s; and a final 10 min at 72°C.

The PCR products were purified using a QIA quick TM PCR purification kit (QIAGEN, Hilden, Germany) and sequenced on an ABI PRISM TM 377 automatic sequencer (Perkin Elmer, USA) at the Mission Biotech, China. Multiple sequence fragments were obtained by sequencing with different primers for each gene and individual. We examined the original chromatograms of each sequence to avoid reading errors and aligned the same gene sequence by eye using Bioedit software (Hall, 1999). The complete

Table 1. Summary of genetic diversity in *Callitettix versicolor* based on mtDNA (*COI* + *Cytb* + *ND5*). Abbreviations of populations (Code), Sample size (*n*), number of haplotypes (*nh*), nucleotide diversity (π), haplotype diversity (*h*), Fu's F_S and Tajima's *D* were estimated based on the mitochondrial DNA. Genetic diversity was only calculated for locations with more than two haplotypes. * $P < 0.05$, ** $P < 0.01$, *** $P < 0.001$.

Population Location	Code	Altitude (m)	Latitude	Longitude	<i>n</i>	<i>nh</i>	π	<i>h</i>	Fu's F_S	Tajima's <i>D</i>
Western lineage	–	–	–	–	19	9	0.00149	0.678	–2.481*	–1.431*
Yongping, Yunnan	YN1	1130.0	25.464543°N	99.540984°E	15	9	0.00188	0.8	–1.530*	–2.351***
Dali, Yunnan	YN	827.3	25.591601°N	100.229757°E	4	3	0.00151	0.833	0.961	–0.817
Eastern lineage	–	–	–	–	135	53	0.00188	0.903	–2.247*	–34.492*
E1 sublineage	–	–	–	–	18	8	0.00106	0.804	–1.298	–1.77
Anqing, Anhui	AQ	260.0	30.824581°N	115.948155°E	10	6	0.00243	0.778	0.676	–1.296
Huanggang, Hubei	HB1	307.3	30.932373°N	115.481022°E	10	5	0.00093	0.667	–0.432	–1.73
E2 sublineage	–	–	–	–	117	45	0.0015	0.87	–	–34.510*
Zhaotong, Yunnan	YN2	731.1	27.836898°N	103.978387°E	5	3	0.00198	0.7	2.141	–0.927
Yongchuan, Chongqing	CQ	274.2	29.312110°N	105.916357°E	10	4	0.00163	0.644	2.158	–1.537
Yibin, Sichuan	SC1	372.2	28.742553°N	104.552608°E	10	5	0.00196	0.8	1.329*	–1.821*
Dazhou, Sichuan	SC3	394.4	31.546392°N	107.647507°E	10	2	0.00009	0.2	–1.347	–1.112
Zunyi, Guizhou	GZ3	864.3	27.914838°N	107.222275°E	5	2	0.00026	0.6	0.626	1.225
Zunyi, Guizhou	GZ5	400.7	28.188317°N	105.987077°E	5	4	0.00327	0.9	1.159	–0.076
Shiyan, Hubei	HB4	301.1	32.294820°N	110.038169°E	5	3	0.00052	0.7	–0.186	–1.048
Wugang, Henan	HN1	143.3	33.283295°N	113.519598°E	5	4	0.00319	0.9	1.116	–0.267
Nanling, Guangdong	GD1	556.1	24.775906°N	113.275952°E	5	2	0.0019	0.4	4.483	–1.2
Nanning, Guangxi	GX1	124.9	23.226323°N	109.126187°E	5	4	0.00086	0.9	–1.012	–1.124
Guilin, Guangxi	GX2	136.1	24.814503°N	110.421868°E	5	4	0.00069	0.9	–1.405	–1.094
Chongzuo, Guangxi	GX3	119.9	22.345973°N	106.887118°E	5	2	0.00026	0.6	0.626	1.225
Henyang, Hunan	HUN1	64.9	26.847683°N	112.400198°E	5	2	0.00034	0.4	1.04	–0.973
Shaoyang, Hunan	HUN3	241.1	27.165788°N	110.922983°E	5	4	0.00069	0.9	–1.405	0.699
Xianning, Hubei	HB2	51.7	29.570107°N	114.055792°E	5	2	0.00034	0.4	–0.954	–0.973
Anlu, Hubei	HB3	94.8	31.286045°N	113.483376°E	5	1	–	–	–	–
Anshun, Guizhou	GZ1	1124.8	25.904382°N	105.550663°E	5	4	0.00172	0.9	0.134	–1.193
Tongren, Guizhou	GZ2	362.9	27.258595°N	108.895588°E	5	3	0.00069	0.7	0.276	0.699
Sandu, Guizhou	GZ6	418.8	25.938873°N	107.867300°E	5	3	0.00043	0.8	–0.475	0.243
Huaihua, Hunan	HUN2	260.0	27.480980°N	109.655437°E	5	2	0.00052	0.6	1.688	1.459

sequences were then assembled using Seqman (Swindell and Plasterer, 1997). The DNA sequences were submitted to GenBank with accession numbers KT891432–KT891585 (*COI*), KT891586–KT891739 (*Cytb*), and KT891740–KT891893 (*ND5*).

We developed 11 pairs of microsatellite polymorphic markers (Supplementary Table S1) using an enrichment protocol following the procedure of Butcher (Butcher et al., 2000) with a slight modification. We genotyped 375 samples from 19 sample sites (Table 3; the YN, GZ3, GZ6, GD1 and HUN1 sample sites were dropped for yielding fewer than five samples). The microsatellite loci were amplified in PCR reactions (10 μ l total volume), each containing 0.5 μ l DNA, 0.5 μ l primers, 5 μ l dNTP Mixture (Tiangen, Beijing, China) and 3.5 μ l deionized water (Tiangen, Beijing, China). The forward primer for each set was fluorescently labeled with one of the dyes TAM, FAM or HEX. PCR conditions were as follows: denaturation at 94°C for 4 min; followed by 40 cycles at 94°C for 40 s, annealing temperature (48°C to 65°C for different loci) for 40 s; and 72°C for 40 s; and a final 10 min at 72°C. All loci were successfully amplified and sequenced with no evidence of null alleles. Fragment lengths were analyzed with reference to the internal size marker GENESCAN-500 ROX (Applied Biosystems) and scored using GENEMARKER 3.7 (SoftGenetics). A total volume of 10 μ l was used for genotyping, composed of 1 μ l sample, 0.5 μ l internal size marker and 8.5 μ l deionized formamide, with 3 min 95°C denaturation and 2 min in an ice-bath. All electropherogram traces were checked manually.

Genetic polymorphism

For the mtDNA sequences (*COI* + *Cytb* + *ND5*), we calculated the number of haplotypes (*nh*), haplotype diversity (*h*) and nucleotide diversity (π) for each population. The McDonald and Kreitman test (McDonald and Kreitman, 1991) was used to examine the selective neutrality of the protein-coding fragments of mtDNA. Two additional neutrality tests, Fu's F_S (Fu, 1997) and Tajima's D (Tajima, 1989), were used to detect departures from the mutation-drift equilibrium that would indicate changes in historical demography and the effect of natural selection. All the tests were implemented in DnaSP 4.0 (Rozas et al., 2003).

For the microsatellite data, parameters such as observed heterozygosity (H_O), expected heterozygosity (H_E), total number of alleles per locus (N_A), allelic richness (A_R), and inbreeding coefficients (F_{IS}) were calculated with FSTAT 2.9.4 (Goudet, 2001). Significant deviations from the Hardy-Weinberg equilibrium after adjusting the significance (α) level for the number of pairwise comparisons of populations and loci were calculated with ARLEQUIN 3.5 (Excoffier et al., 2007) with 1000 dememorizations in one million Markov chain approximations.

Phylogeography and population structure

MrBayes 3.1 (Ronquist and Huelsenbeck, 2003) was used to reconstruct the Bayesian inference (BI) trees. Two congeneric species, *Callitettix braconoides* and *Callitettix biformis*, were used as outgroups, both being closely related to *C. versicolor* (Wang et al., 2015). On the basis of the Akaike Information Criterion (AIC), the GTR + I + G model was selected as the optimal model of nucleotide substitutions using jModeltest 0.1.1 (Posada, 2008). We ran MCMC chains for 10 million generations and trees were sampled every 10,000 generations. The MCMC searches were terminated after the convergence diagnostic potential scale reduction factor reached 1, indicating the convergence of separate runs. The initial 1000 samples were discarded as burn-in, and the Bayesian consensus tree was obtained with the posterior probability (PP) calculated for each branch. Minimum-spanning networks were derived using Network 4.610 (Bandelt et al., 1999) with the median-joining approach.

For microsatellite genotypes, STRUCTURE 2.3.2 (Pritchard et al., 2000) was implemented to infer the number of genetically distinct groups using a Bayesian clustering method. The program was run under the admixture model without prior population information

for 50 million iterations, with a burn-in period of 500,000 iterations. We conducted 10 replicates for each value of K from 1 to 10. The most likely number of groups was determined using the ΔK method following Evanno's guide (Evanno et al., 2005) in Structure Harvester (Earl and Vonholdt, 2012). After the optimal value of K was chosen, the associated 10 MCMC replicates were aligned under the greedy algorithm of CLUMP 1.1.2 (Jakobsson and Rosenberg, 2007) and plotted in DISTRUCT 1.1 (Rosenberg, 2004). We followed Weisrock's criterion (Weisrock et al., 2010) in discarding individual membership coefficients with posterior probabilities < 0.05 and assigned corresponding values proportionally to other membership coefficients, so that the coefficients for each individual still summed to one.

We estimated pairwise sequence divergence values of mtDNA between populations in MEGA5 (Tamura et al., 2011) and genetic identity and genetic distance among populations from the microsatellite data using POPGENE (Yeh et al., 1997). Molecular variance (AMOVA) (Excoffier et al., 1992) of mtDNA and microsatellite data were analyzed to examine the hierarchical partition of genetic variation among regions and populations using ARLEQUIN 3.5. The statistical significance of covariance of both types of data associated with each hierarchical level was calculated from 1000 permutations.

Divergence time estimate

We estimated the divergence times in BEAST1.4.6 (Drummond and Rambaut, 2007) using the molecular clock based on Maekawa and López-López (Maekawa et al., 2001; López-López et al., 2015). An uncorrelated log normal relaxed clock (Drummond et al., 2006) was applied to the mtDNA sequences. The average genetic distance of the mtDNA (*COI* + *Cytb* + *ND5*) was 1.38 times greater than the net average genetic distance of *COI* alone. To obtain a more conservative estimate of the divergence time in *C. versicolor*, we calibrated the substitution rate (0.0145 and 0.0244 per site per million years) of the combined mtDNA according to a standard insect *COI* substitution rate of 0.0105 per site per million years and a common mutation rate of 0.0177 per site per million years (Simon, 2006; Papadopoulou et al., 2010). We selected the best-fit model of nucleotide substitution for each locus using the AIC in the jModelTest 0.1.1. We ran MCMC chains for 50 million generations (sampling every 5000 generations and discarding the first 20% as burn-in). Chain convergence was assessed by effective sample size (ESS) values of the parameters in TRACER 1.5 (Jakobsson and Rosenberg, 2007). The final tree was summarized using the program TreeAnnotator in BEAST.

Historical demography

We used three methods to reconstruct the demographic histories of *C. versicolor*. First, two statistics, Fu's F_S and Tajima's D , were used to assess whether nucleotide polymorphisms deviated from expectations assuming neutrality. We calculated these two statistics for each population and lineage. Statistical significance was tested with 10,000 coalescent simulations in ARLEQUIN 3.5. Secondly, mismatch analysis was conducted using ARLEQUIN 3.5. Finally, we used Bayesian skyline plots (BSP; Heled and Drummond, 2008) implemented in BEAST 1.4.6 to assess historical changes in effective population sizes. BSP analyses were conducted separately for the two lineages with the same clock model, substitution model and substitution rate used to estimate divergence time. An uncorrelated lognormal relaxed clock was used for the mtDNA sequences. All analyses were run for 50 million iterations with trees sampled every 5000 generations. The initial 10% of the run was discarded as burn-in. The ESS for the posterior distribution of estimated parameter values was assessed in TRACER 1.5.

Ecological niche modeling

We calculated the geographical distributions of *C. versicolor*

during three time periods (the Present Day, the Last Glacial Maximum (LGM) and the Last Interglacial (LIG)) using MaxEnt 3.3.2 (Phillips et al., 2006) and incorporating 19 bioclimatic variables (Supplementary Table S2). MaxEnt was used because the program is robust to low sample sizes (Pearson et al., 2007). Climate data were downloaded from WorldClim (Hijmans et al., 2005; <http://www.worldclim.org/>), including annual trends, seasonality and extremes of temperature and precipitation (Supplementary Table S2). These bioclimatic variables were at a resolution of 2.5 arc-minutes. We compared the pairwise correlations between variables with Pearson's correlation coefficient (r ; Pearson et al., 2007) to minimize model over-fitting (Supplementary Table S10). When two variables were strongly correlated ($r > 0.9$), we chose the one being more biologically meaningful for the species. In total, 12 bioclimatic variables were used in the subsequent analyses, i.e., annual mean temperature, mean diurnal range, isothermality, temperature seasonality, max temperature of warmest month, mean temperature of wettest quarter, annual precipitation, precipitation of wettest month, precipitation of driest month, precipitation seasonality, precipitation of warmest quarter, precipitation of coldest quarter. The occurrence data of *C. versicolor* included our sampling sites and documented historical records. Only localities with geo-referenced data of longitude and latitude were used. We used Google Earth (<http://earth.google.com/>) to confirm the records, and dropped sites that were close to one another (less than 0.1°) to reduce the effect of spatial autocorrelation. A total of 85 localities were used in the final analysis (Supplementary Table S9). These data covered almost the entire distribution area of *C. versicolor* in South China. Eighty percent of the occurrence data were randomly selected for model construction and the remaining twenty percent were used for model testing. We used the default setting of the convergence threshold (10^{-5}) and limited the number of maximum iterations to 2000 and the number of replicates to 10 (Wang et al., 2013). The output format was set to be logistic. This output ranged from 0 to 1 to quantify the probability of environmental conditions suitable for the species in different sites. Model performances were assessed by averaging areas under the receiver operating characteristic curves (AUC) and the binomial probabilities over ten replicate runs.

RESULTS

Genetic polymorphism

A total of 2321 bp of mtDNA (*COI* 887 bp, *Cytb* 645 bp, *ND5* 789 bp) was obtained. The mtDNA of all the sequenced samples contained 146 polymorphic sites, 88 of them being parsimony-informative. These polymorphic sites comprised 62 unique haplotypes, 47 of which occurred only once. Eleven of these were shared among individuals within the same population: Hap 8, 16, 20, 21, 27, 31, 33, 37, 44, 47 and 53. Hap 53 showed the highest frequency, occurring in 11 samples. Four haplotypes were shared among neighboring populations: Hap 3, 7, 12 and 25. Hap 3 and Hap 25 were present in six and three samples from two populations, separately. Hap 7 was present in 38 samples from 12 neighboring populations and Hap 12 in 15 samples from six neighboring populations (Supplementary Table S3). In addition to GD1, all the populations containing Hap 7 were in the north of South China, while all those containing Hap 12 were in the south (Fig. 1, Fig. 2).

Within sampling locations, haplotype diversity (h) values ranged from 0.200 to 0.900, and nucleotide diversity (π) ranged from 0.00009 to 0.00327. The McDonald–Kreitman test showed no significant deviation from neutrality for the three mtDNA coding segments ($P > 0.05$, with Fisher's exact test). The mtDNA haplotype diversity (h) was moderate to

high ($h = 0.678\text{--}0.903$) in the Western and Eastern lineages, while nucleotide diversity was quite low ($\pi = 0.00106\text{--}0.00150$, Table 1).

For microsatellite data, there were 1–13 alleles per locus across all populations; the observed (H_o) and expected heterozygosity (H_e) ranged from 0.05 to 0.92 and 0.05 to 0.95, respectively. There was no evidence of linkage disequilibrium after sequential Bonferroni correction ($P < 0.001$). Deviations from HW equilibrium were observed at some loci of 15 locations (the loci deviated from HW in different population ranged from 0 to 6; Supplementary Table S4). The percentage of deviated loci is 17.2% among all the loci. We calculated both kinds data (with or without deviated loci) and found that the results were similar (Table 3, Supplementary Table S5), so we retained the full data set for subsequent analyses.

Phylogeography and population structure

The Bayesian phylogeny of *C. versicolor* indicated that the mtDNA is composed of three main geographically structured lineages (W, E1 and E2). Two main lineages (E and W) with a deep phylogenetic split were well supported (Bayesian posterior probabilities: 1.00, Fig. 2). The W lineage only occurred in a narrow region (YN and YN1) of the southwest of China (east edge of Tibetan plateau). The geographically widespread lineage (E) was clearly composed of two geographically and phylogenetically distinct sub-lineages, E1 and E2, supported by moderate Bayesian posterior probabilities (0.73, Fig. 2). The E1 sub-lineage was distributed only from the eastern edge of South China. The latter contained two distinct lineages (E2-1, E2-2) co-distributed over most of central South China, indicating a phylogeographical pattern expected for a high gene flow species with relatively small population sizes not separated by a long-term geographical barrier.

Network analysis demonstrated that the W and E2 (E2-1 and E2-2) lineages contained star-like networks (Fig. 2). In the W lineage, the dominant haplotype, Hap 53, occurred in 11 samples from only one single population (YN1). In the E lineage, the two dominant haplotypes, Hap 7 and Hap 12, were present in the E2-1 and E2-2 sub-lineages, separately. Hap 7 occurred in 38 samples distributed across 12 populations (CQ, GD1, GZ2, GZ3, GZ5, GZ6, HB4, HN1, HUN2, SC1, SC3, and YN2; Table S3), while Hap 12 occurred in 15 samples distributed across six populations (GX1, GZ1, GZ6, HB2, HUN1, and HUN3; Table S3). In addition to the three dominant haplotypes (Hap 53, 7 and 12), only two (Hap3 and Hap 25) were shared between two populations. Hap3 of E1 located in AQ and HB1 and Hap 25 of E2 located in GZ2 and HUN2 (Fig. 1, Table S3).

The mtDNA results in AMOVA indicated that the largest variation (90.59%, d.f. = 1) was between regions (W and E lineages; Table 2). For the AMOVA of microsatellite data, the variations were largest within individuals (67.23%, d.f. = 393) and smaller within populations (5.06%, d.f. = 373). The variation among groups (15.59%, d.f. = 6) was higher than within groups (12.12%, d.f. = 13). All the variations were statistically significant ($P < 0.001$, Table 4). STRUCTURE analyses of microsatellite data suggested four distinct genetic clusters (DeltaK = 8.99, Fig. 3, Table S4). The first of these (G1) comprised individuals from one population (YN1) of the

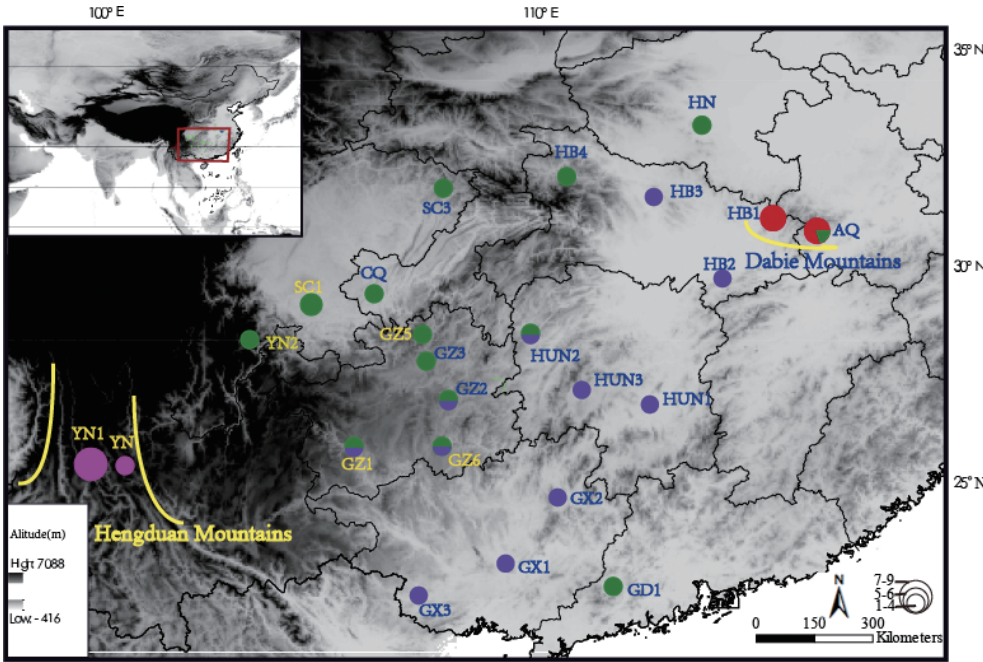


Fig. 1. Map of sampling locations for *Callitettix versicolor*. Different colors correspond to different sublineages reconstructed by MrBayes 3.1 (W: rose red and E1: red, E2-1: green, E2-2: purple). The size of the pies represents the number of samples from the corresponding locality. Abbreviations of populations are detailed in Table 1. The yellow lines denote approximate geographical boundary (mountains). The distribution ranges were shown at the upper-left corner. The map was drawn using ArcGIS v10.1 (ESRI, CA, USA) and Adobe Illustrator CS5v15.0.0 (Adobe Systems Inc., San Francisco, CA).

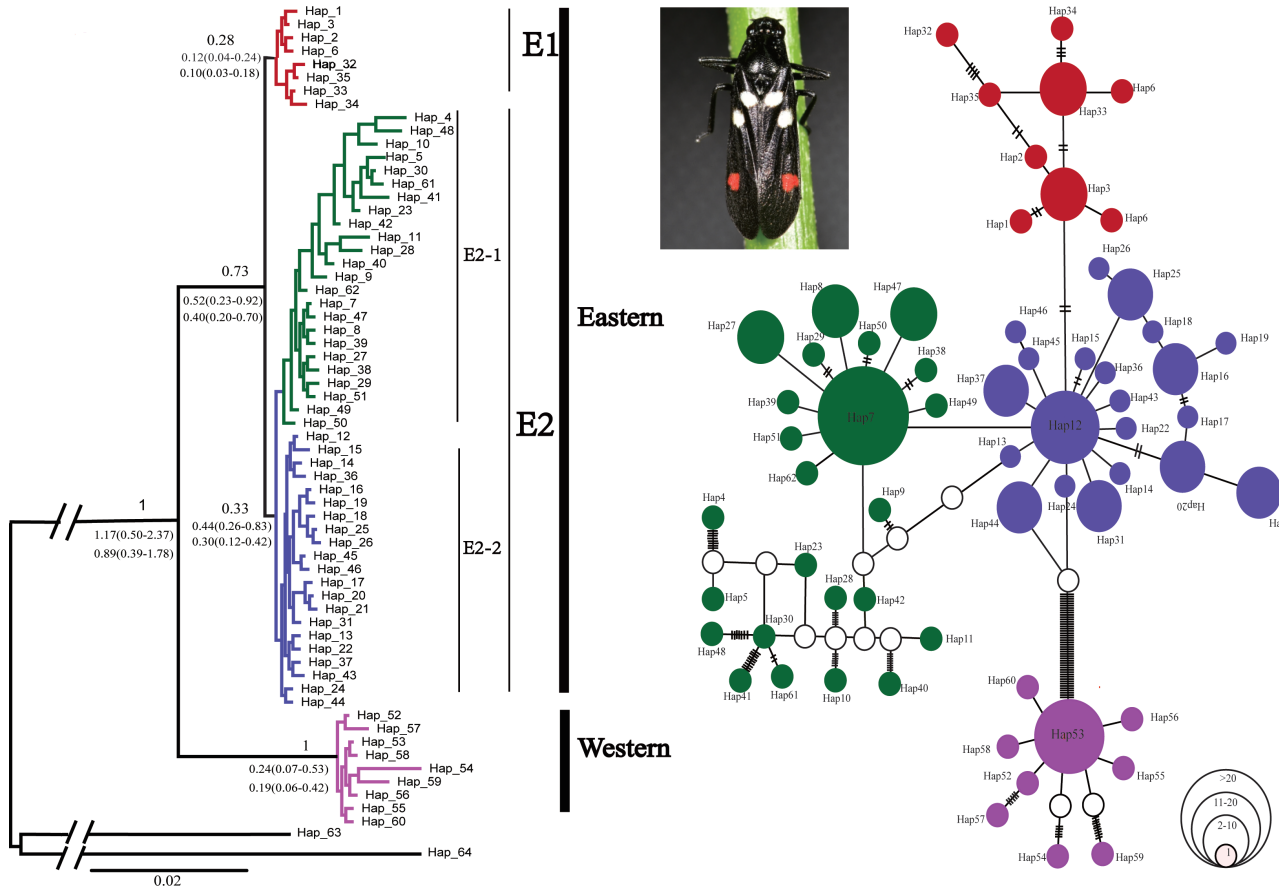


Fig. 2. Bayesian phylogenetic tree (left) and the median-joining network (right) of mtDNA (*COI* + *Cytb* + *ND5*) haplotypes for *Callitettix versicolor*. In the Bayesian phylogenetic tree, Bayesian posterior probabilities values are above the branches. Estimates of divergence time based on two mutation rates with 95% highest posterior densities are shown as numbers below branches. In the network, sizes of circles indicate the haplotype frequencies. Network branches linking the cycles indicate one mutation step; two or more mutations are represented by slashes crossed with the network branches. The white circles are hypothetical missing intermediates. Colors denote different lineages in Bayesian phylogenetic tree and network are the same as in Fig. 1.

Table 2. The analysis of molecular variance (AMOVA) based on the mtDNA (*COI* + *Cytb* + *ND5*). d.f., degrees of freedom. **denotes significance at $P < 0.01$.

Source of variation	d.f.	Sum of squares	Variance component	Variation (%)	Fixation indices
Between regions	1	852.18	24.85968	90.59	FCT : 0.90587**
Among populations within regions	2	79.737	0.95677	3.49	FSC : 0.37039**
Within populations	150	243.96	1.6264	5.93	FST : 0.94074**
Total	153	1175.877	27.44285	–	–

Table 3. Summary of mean genetic variation at 11 microsatellite loci for *Callitettix versicolor* populations. H_O , observed heterozygosity; H_E , expected heterozygosity; N_A , total number of alleles; A_R , allelic richness; F_{IS} , inbreeding coefficients. See Table 1 for abbreviations of sampling populations and Table S3 for information details of 11 microsatellite locus.

Sampling location	N	H_E	H_O	N_A	A_R	F_{IS}
YN1	19	0.661	0.569	6.091	5.746	0.161
AQ	20	0.592	0.550	5.545	5.203	0.251
HN1	20	0.455	0.411	3.818	3.547	0.017
SC1	20	0.511	0.490	4.000	3.759	-0.015
HB1	20	0.655	0.645	5.545	5.267	0.024
YN2	20	0.412	0.405	3.273	3.143	-0.067
GX1	20	0.683	0.531	6.455	5.999	0.275
GX2	16	0.615	0.556	4.636	4.451	-0.032
HB3	20	0.547	0.585	4.000	3.823	0.088
HUN2	20	0.665	0.585	6.091	5.681	0.165
CQ	20	0.541	0.435	4.727	4.439	0.080
GX3	20	0.756	0.695	8.818	8.818	0.132
SC3	20	0.512	0.475	5.364	5.018	0.133
HUN3	20	0.671	0.563	6.727	6.326	0.163
GZ1	20	0.656	0.485	6.000	5.611	0.284
HB2	20	0.644	0.570	6.636	6.167	0.119
HB4	20	0.595	0.493	6.273	5.875	0.004
GZ2	20	0.694	0.622	6.909	6.391	0.091
GZ5	20	0.465	0.505	4.273	4.015	-0.157

Table 4. The analysis of molecular variance (AMOVA) of different geographical populations of *Callitettix versicolor* based on the microsatellite data. d.f. degrees of freedom. **denotes significance at $P < 0.01$.

Source of variation	d.f.	Sum of squares	Variance component	Variation (%)	Fixation indices
Among groups	6	589.475	0.6896	15.59	FIS: 0.07002**
Among populations within groups	13	319.062	0.53608	12.12	FSC: 0.14355**
Among individuals within populations	373	1276.577	0.22395	5.06	FCT: 0.15587**
Within individuals	393	1169.000	2.97455	67.23	-FIT: 0.32766**

W lineage. The other three (G2, G3 and G4) largely corresponded to the mitochondrial haplotype lineages (E1, E2-2, and E2-1) reconstructed in phylogenetic and network analyses, respectively. G2 consisted of three populations (AQ, HB1, and HB3); G3 included six populations (HUN3, HB2, GZ1, GX1, GX2, and GX3) and G4 included nine (HN1, SC1, HUN2, YN2, GZ2, GZ5, CQ, SC3, and HB4) (Fig. 3). In G2, in addition to HB3 belongs to E2-2, the populations

(AQ, HB1) were in the E1 sub-lineage. In G3 and G4, the populations were consisted to E2-2 and E2-1, separately.

In the G1 and G2 clusters, the maximum proportion of ancestry of populations was high (0.9692–0.9867), indicating a single ancestral character; the maximum proportions in G3 (HUN3, 0.4922; GZ1, 0.7003) and G4 (HUN2, 0.5078; GZ2, 0.6485) were lower, indicating more than one ancestral character (Fig. 3, Table S6). The multiple ancestral populations (GZ1, GZ2, HUN2, HUN3) from G4 and G3 were similar to the populations (GZ1, GZ2, GZ6 and HUN2) with haplotypes shared between E2-1 and E2-2. Interestingly, these populations developed a narrow overlapped zone at Guizhou province and west area of Hunan province neighboring E2-2 and E2-1, the hybrid zone (Fig. 1).

Divergence time

The divergence time for the deepest split between the E and W lineages was dated to 1.17–0.89 million years (Mya) (95% HPD for both datings were 0.50–2.37 Mya and 0.39–1.78 Mya). The divergence between the E1 and E2 sub-lineages was traced back to 0.52–0.40 Mya (95% HPD for both datings were 0.23–0.92 Mya and 0.20–0.70 Mya). The divergence time between E2-1 and E2-2 was 0.44–0.30 Mya (95% HPD for both were 0.26–0.83 Mya and 0.12–0.42 Mya) (Fig. 2).

Demographic reconstruction

Fu's F_S and Tajima's D did not reach statistical significance in most inter-population comparisons, but were significantly negative for comparisons between YN1 and the other populations (Table 1). The BSP rejected population stability in the Eastern lineage (including E1, E2-1 and E2-2), but could not reject population stability in the Western lineage (Fig. 4). BSP estimates of the Eastern lineage and E2-1 sub-lineage suggested that the population had expanded approximately tenfold, beginning around 0.075 Mya, with no evidence of contraction afterwards. This demographic expansion coincided with the transition from the LIG to the LGM. However, the expansions of E1 and E2-2 are not as evident as E2-1 lineage (Fig. 4).

Ecological niche modeling

The ecological niche models for *C. versicolor* (Fig. 5) had excellent predictive power, with an average training AUC of 0.998 and low binomial probabilities ($P < 0.0001$) (Swets, 1988). The predicted present distribution of *C. versicolor* was similar to that of the LIG period and more extensive than it had been in the LGM period. The predicted distribution of the Western lineage reached its respective largest and smallest extents during the LIG and LGM periods, respectively. For the Eastern lineage, the predicted present distribution is more similar to that of the LIG than the LGM period. However, the predicted present distribution of *C. versicolor* suggests a greater expansion to east China than during LIG or LGM. There is currently a narrow area of contact between the two lineages. Two lineages kept contact during the LIG and apart during LGM period according

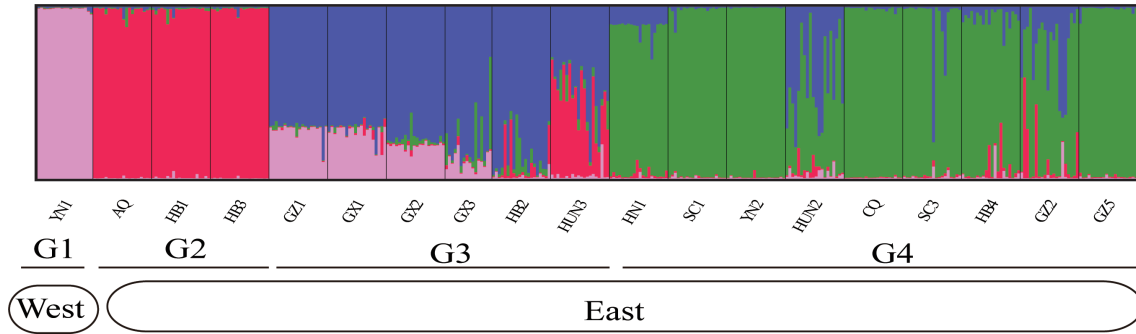


Fig. 3. Estimated population structure of *Callitettix versicolor* based on STRUCTURE analysis of microsatellite data. Four genetic clusters are recognized. Bars represent single specimens from the regions depicted at the bottom. Abbreviations of populations are detailed in Table 1.

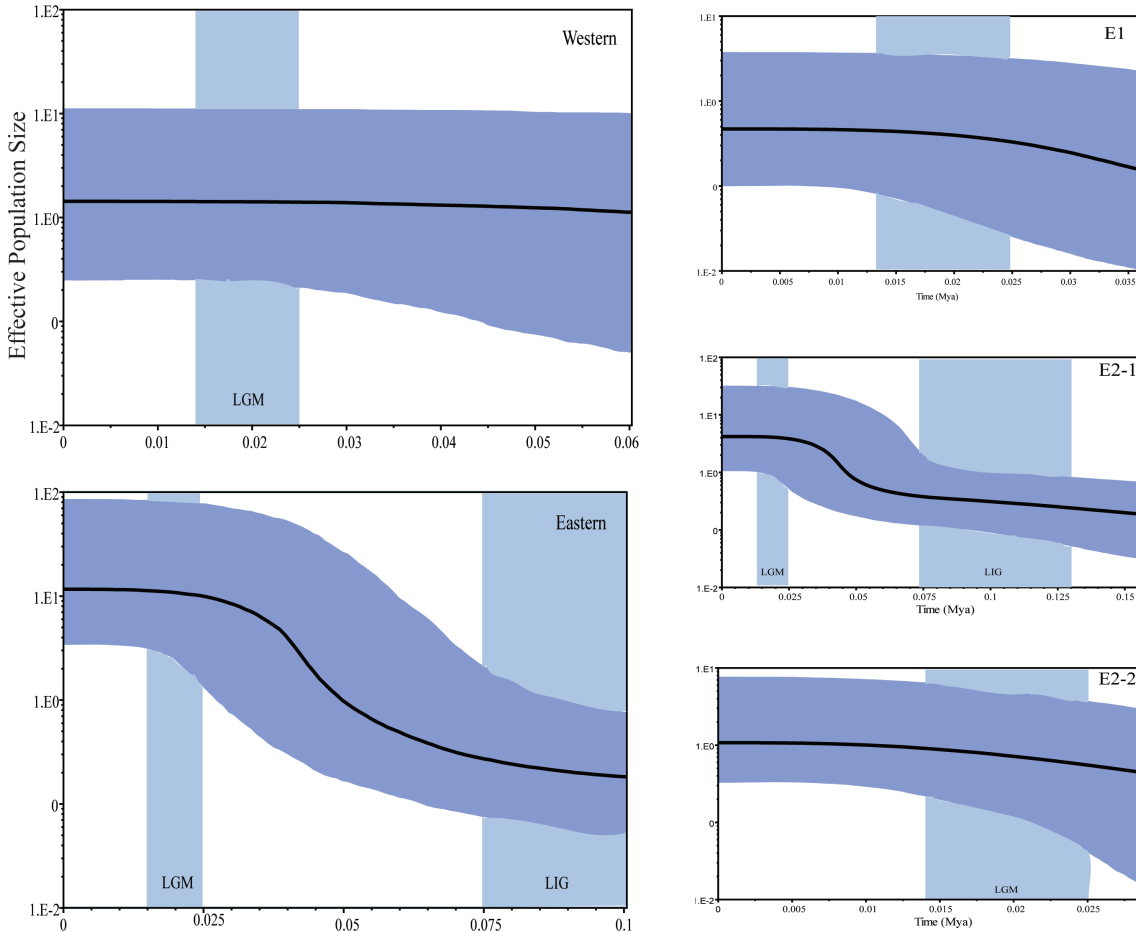


Fig. 4. Bayesian skyline plots (BSP) representing historical demographic trends of the Western and Eastern lineages (E1, E2-1 and E2-2) of the *Callitettix versicolor*. Time (Mya) is shown along the x-axis, and the scaled effective population size is shown along the y-axis. The shaded areas represent 95% highest posterior densities (95% HPD). LGM represents the Last Glacial Maximum, and LIG represents the Last Interglacial.

to this area.

DISCUSSION

Our phylogeographic study suggests that the population genetic structures of *C. versicolor* have been strongly affected by geographic barriers. The mtDNA data revealed two distinct lineages (Western and Eastern) that are consistent with the biogeographical regions separated by the

Hengduan Mountains. The Eastern lineage was subdivided into two sub-lineages, E1 and E2, consistent with the geographically separated central and eastern sub-regions of the Dabie Mountains. E2 was further subdivided into two sub-groups, E2-1 and E2-2, with a hybrid zone in Hunan and Guizhou provinces where their populations were contiguous. The genetic structures constructed by mtDNA were corroborated by four clusters (G1–G4) of microsatellite data. The

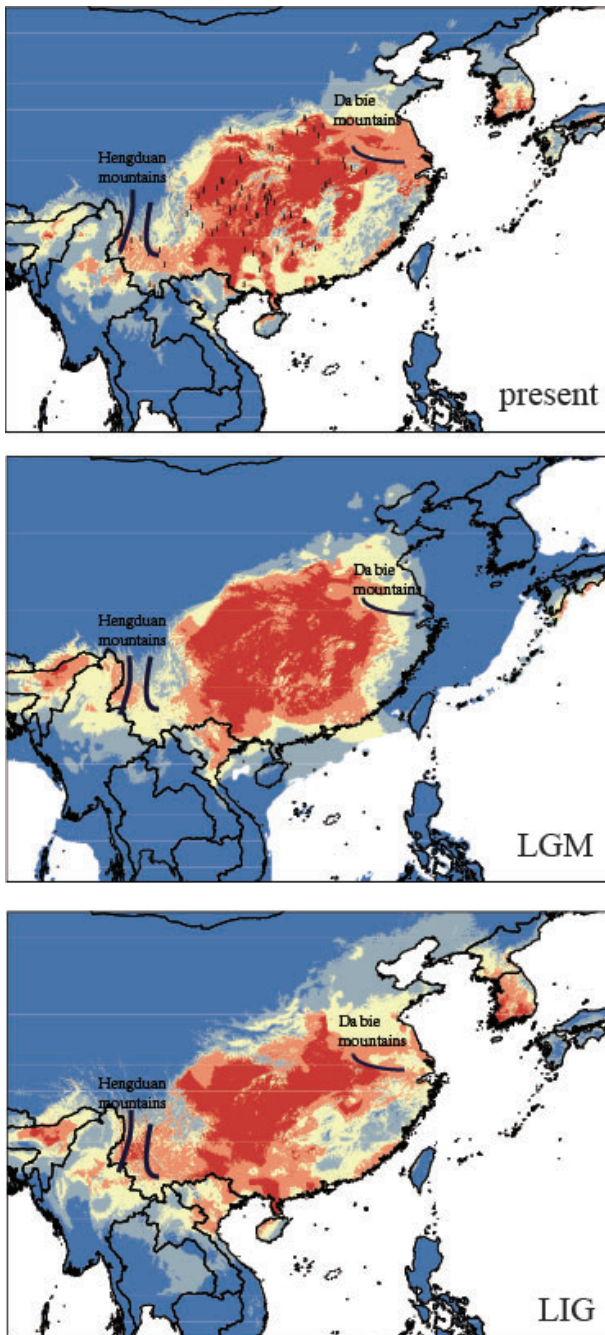


Fig. 5. Ecological niche models for *Callitettix versicolor* in three periods, i.e., the Present Day, the Last Glacial Maximum (LGM) and the Last Interglacial (LIG). Black dots represent the localities used to build the ecological niche models. The black lines denote approximate geographical boundary (mountains). Warmer colors show areas with better predicted conditions. Different colors correspond to different fitting indices, with high in red and low in blue.

divergence time estimates between the Western and Eastern lineages were 1.17 (0.50–2.37)–0.89 (0.39–1.78) Mya, indicating that they diverged on two different geographic and temporal scales. The historical demography of the Eastern lineage showed continuous population growth after the Last Interglacial (LIG) and remained stable during the Last Glacial Maximum (LGM) period. However, the

Western lineage remained largely unchanged during the glacial and inter-glacial periods. This conclusion is consistent with our ecological niche models, which suggested that the historical demography of *C. versicolor* is likely related to the paleoclimate of South China.

Phylogeographical structure

The phylogeography of *C. versicolor* indicated a long history of geographical isolation between southwest and southeast China. Three well-supported reciprocally monophyletic mtDNA phylogroups were allopatrically distributed and separated by mountain barriers (Figs. 1 and 2). The populations from southeast China formed a clade (E1 sub-lineage) that was sister to a clade comprising individuals from central South China (E2 sub-lineage). The populations from west of the Hengduan Mountains, in southwestern China, formed a third, well-supported, basal clade (Western lineage).

The effects of long-term mountain barriers on geographic isolation have been demonstrated in many mountain species (Li et al., 2012; Liu et al., 2015). In South China, Qu (Qu et al., 2011) using mitochondrial data detected two deep divergence lineages (north-eastern and southern) of *Garrulax elliotii* in the eastern Himalayas, i.e., the Hengduan Mountains area, during the interglacial periods (LIG). Moreover, the isolation function of the Hengduan Mountains was also apparent in many other species including the green-backed tit (*Parus monticolus*) and the alp frog (*Nanorana parkeri*) (Li, 1989; Zhang et al., 2009; Li et al., 2012; Wang et al., 1998; Liu et al., 2015). The steep Hengduan Mountains, located at the edge of southwest China, lie between the Western and Eastern lineages, are likely to have served as a geographic barrier for them. Previous related research paid more attention to the effects of isolation on mammals and amphibians rather than insects. The present study seems to be the first to identify the isolation function of the Hengduan Mountains for a phytophagous insect.

Unlike the Hengduan Mountains, the best-established geographic species barrier, less attention has been paid to the Dabie Mountains of southeast China, which have a lower altitude and had moderate temperatures during the ice age. In this study, the Dabie Mountains were identified as a geographic barrier between the E1 and E2 sub-lineages, a finding consistent with a recent study by Zhang and colleagues of *Tomocerus* (Collembola, Tomoceridae), a small arthropod characterized by a jumping organ (furcula) on the ventral side of the fourth abdominal segment (Zhang et al., 2014). The two studies identified the Dabie Mountains as a long-term biogeographical barrier, suggesting that more attention should be paid to the Dabie Mountains in future.

Multiple data studies in phylogeography have become a popular trend. In the present study, the topology of the mtDNA gene tree was similar to the microsatellite population structure (Figs. 2 and 3). This structure, which included 11 microsatellite loci (Fig. 3), revealed four clusters, G1 to G4. They corresponded to the Western lineage, E1, E2-2 and E2-1 sub-lineages of the mtDNA gene tree. Moreover, the area where mtDNA haplotypes overlapped was reflected in the microsatellite results. The hybrid zone was in Guizhou and Hunan provinces, the area neighboring both E2-1 and E2-2, which may have facilitated gene contact between the

two sub-lineages.

Compared with the microsatellite data, the mtDNA gene tree presents a clearer topology and demands a lower effective population size, so it promotes faster lineage sorting. The high fitness of general primers is another advantage of mtDNA. As we know, microsatellite loci are characterized by high polymorphism, offering a possible window into recent gene contacts among populations (Slatkin, 1995) and permitting inferences about recent contact histories within specific populations (Carter et al., 2010), which cannot be achieved using mtDNA. In this study, we found that haplotype mix in mtDNA have only happened in four nearby populations. However, in microsatellites data, over nine populations have more than one ancestry. The more gene contact in microsatellites data may be related to the recent contact of *C. versicolor*. Considering the different features of mtDNA and microsatellites, we reinforced the importance of incorporating multiple data types in reconstructing the historical relationships among species and populations.

Effect of Pleistocene climate on divergence

In addition to geographic complexity and environmental heterogeneity, the Pleistocene climate is also likely to have shaped the genetic structures of populations within a species (Li, 1989; Zhang et al., 2009). Previous studies indicated that Pleistocene climate changes had profound effects on the divergence of species in southwest China (Qu et al., 2011; Zhao et al., 2012). In the present study, two distinct lineages with a large phylogenetic split (Eastern and Western) were identified in *C. versicolor* from both mtDNA and microsatellite data. Divergence time estimates indicated that the Eastern and Western lineages diverged about 1.17–0.89 Mya. This divergence time is similar to that of the short-tailed pit viper (*Gloydus brevicaudus*; 1.068 Mya; Ding et al., 2011) and the black-spotted frog (*Pelophylax nigromaculatus*; 0.92 Mya; Zhang et al., 2008), both also ectothermic creatures that are distributed over a geographical area and altitudinal range similar to that of *C. versicolor*. This divergence time falls within the mid-late Pleistocene (Ruddiman and Kutzbach, 1989) and is probably associated with the climatic changes known to have occurred after the Mid Pleistocene Quaternary glaciations, including the Gunz glaciation (1.2–0.9 Mya), which may have caused changes in distribution and subsequently led to allopatric isolation and lineage splits (Huang et al., 2005). Therefore, the results indicate a long history of population isolation, and Pleistocene climatic fluctuations are probably associated with species diversification and the formation of lineages.

Demographic history

In South China, which did not experience large-scale glaciations, the historical demographics of species show a different trend from those in Europe and North America (Hewitt, 1996, 2000, 2004; Mahmut et al., 2002; Chen et al., 2008; Cao et al., 2012; Jing et al., 2014; Ye et al., 2014). Our historical demographic analyses show that the population size of the Western lineage from the southwest of China remained relatively stable throughout the glaciation period (Fig. 4), in contrast to the twite (*Carduelis flavirostris*) and black redstart (*Phoenicurus ochruros*) distributed in the similar area, which experienced population expansion following

the retreat of the extensive glaciation (0.5–0.175 Mya; Qu et al., 2010). This expansion could be because the milder climate of the Tibetan Plateau eastern margin during the glaciation period mitigated the demographic stresses for these species, making the historical population sizes constant (Yuan et al., 2004; Kelly et al., 2006). In addition to climatic changes, various behavioral and ecological characteristics of the organism, including dispersal capacities, habitat preference, and altitude specificity could also have helped to shape its phylogeographical structures. *C. versicolor* is sensitive to habitat temperature and humidity, so it cannot live above 1200 m altitude. The low dispersal ability of *C. versicolor* is therefore likely to be greatly limited by long-term geographic barriers such as the Hengduan Mountains.

The Eastern lineage was estimated to have undergone population expansion from approximately 75,000 years ago (Fig. 4), earlier than the LGM and associated with the pre-LGM period. Similar historical demographical expansion has been observed in other East Asian animals (Qu et al., 2011; Wang et al., 2013). Before the LGM, the warm and humid climate of inter-glaciation could have facilitated the population expansion of *C. versicolor*. During the LGM, South China did not experience large-scale glaciations, due to the blocking of cold winds by the Tibetan Plateau. This is different from Europe and North America, which were covered by glaciations during this period. Climate fluctuations, geological restriction, and specific habitat preferences of species may thus all be closely related to the different demographic histories of the Western and Eastern lineages of *C. versicolor*.

The results of the present study clearly reveal the distribution pattern of *C. versicolor* in south China, which is significant for the phylogeography of South China. However, further study is needed to resolve a number of questions. In our study, all the populations composed lineages had a strong correlation to geography except for GD1, which, distinct from other neighboring populations in southern China, shared its haplotype with E2-1 populations rather than E2-2 (Fig. 1). More samples from surrounding areas are needed to resolve this anomaly. We also found in mtDNA data, haplotype of HB3 was in E2-2 sub-lineage, while in microsatellite data, HB3 was clustered in G2. This discrepancy may be attributable to different mutation frequencies in these two types of data; further study is needed to address this question.

ACKNOWLEDGMENTS

We thank Prof. Dr V. B. Meyer-Rochow, Oulu University, Oulu, Finland for revision of this manuscript. We thank Prof. Jin-zhong Fu, Associate Professor, Department of Integrative Biology, University of Guelph for his valuable comments on an earlier version of this manuscript. We also appreciate the help of our colleague Lin-xing Li, and many anonymous farmers who assisted with sample collections. The work described in this paper was supported by the the Cooperative Research Projects in Biodiversity jointly supported by the National Natural Science Foundation of China and the K.T. Li Foundation for the Development of Science and Technology (Grant No. 31561163003), the Ministry of Science and Technology of the People's Republic of China (MOST Grant No. 2011FY120200) and the National Natural Science Foundation of China (Grant Nos. 31372249, 31572298), awarded to APL.

REFERENCES

- Avise JC, Walker D, Johns GC (1998) Speciation durations and Pleistocene effects on vertebrate phylogeography. *Proc R Soc London Ser B* 265: 1707–1712
- Bandelt HJ, Forster P, Rohl A (1999) Median-joining networks for inferring intraspecific phylogenies. *Mol Biol Evol* 16: 37–48
- Butcher PA, Decroocq S, Gray Y, Moran GF (2000) Development, inheritance and cross-species amplification of microsatellite markers from acacia mangium. *Theor Appl Genet* 101: 1282–1290
- Cao MM, Jin YT, Liu NF, Ji WH (2012) Effects of the Qinghai-Tibetan Plateau uplift and environmental changes on phylogeographic structure of the Daurian Partridge (*Perdix dauuricae*) in China. *Mol Phylogenet Evol* 65: 823–830
- Carter M, Smith M, Harrison R (2010) Genetic analyses of the Asian longhorned beetle (Coleoptera, Cerambycidae, *Anoplophora glabripennis*), in North America, Europe and Asia. *Biol Invasions* 12: 1165–1182
- Chen K, Abbott RJ, Milne RI, Tian XM, Liu JQ (2008) Phylogeography of *Pinus tabulaeformis* Carr. (Pinaceae), a dominant species of coniferous forest in northern China. *Mol Ecol* 17: 4276–4288
- Chen X, Liang AP (2012) Laboratory rearing of *Callitettix versicolor* (Hemiptera: Cicadomorpha: Cercopidae), with descriptions of the immature stages. *Ann Entomol Soc Am* 105: 664–670
- Ding LI, Gan, XN, He SP, Zhao EM (2011) A phylogeographic, demographic and historical analysis of the short-tailed pit viper (*Gloydus brevicaudus*): evidence for early divergence and late expansion during the Pleistocene. *Mol Ecol* 20: 1905–1922
- Drummond AJ, Ho SYW, Phillips MJ, Rambaut A (2006) Relaxed phylogenetics and dating with confidence. *PLoS Biol* 4: e88
- Drummond AJ, Rambaut A (2007) BEAST: Bayesian evolutionary analysis by sampling trees. *BMC Evol Biol* 7: 214
- Earl DA, Vonholdt BM (2012) STRUCTURE HARVESTER: a website and program for visualizing STRUCTURE output and implementing the Evanno method. *Conserv Genet Resour* 4: 1–3
- Evanno G, Regnaut S, Goudet J (2005) Detecting the number of clusters of individuals using the software structure: a simulation study. *Mol Ecol* 14: 2611–2620
- Excoffier L, Laval G, Schneider S (2007) Arlequin (version 3.0): an integrated software package for population genetics data analysis. *Evol Bioinform* 1: 47–50
- Excoffier L, Smouse PE, Quattro JM (1992) Analysis of molecular variance inferred from metric distances among DNA haplotypes: application to human mitochondrial DNA restriction data. *Genetics* 131: 479–491
- Fu YX (1997) Statistical tests of neutrality of mutations against population growth, hitchhiking and background selection. *Genetics* 147: 915–925
- Goudet J (2001) FSTAT, a program to estimate and test gene diversities and fixation indices version 2.9.3.2. Available from <http://www2.unil.ch/popgen/softwares/fstat.htm> [Updated from Goudet (1995)]
- Hall TA (1999) BioEdit: a user-friendly biological sequence alignment editor and analysis program for Windows 95/98/NT[C]/Nucleic acids symposium series 41: 95–98
- Heled J, Drummond AJ (2008) Bayesian inference of population size history from multiple loci. *BMC Evol Biol* 8: 1–15
- Hewitt GM (1996) Some genetic consequences of ice ages and their role in divergence and speciation. *Biol J Linn Soc* 68: 247–276
- Hewitt GM (2000) The genetic legacy of the Quaternary ice ages. *Nature* 405: 907–913
- Hewitt GM (2004) Genetic consequences of climatic oscillations in the Quaternary. *Philos Trans R Soc London* 359: 183–195
- Hijmans RJ, Cameron SE, Parra JL, Jones PG, Jarvis A (2005) Very high resolution interpolated climate surfaces for global land areas. *Int J Climatol* 25: 1965–1978
- Huang JP, Lin CP (2010) Diversification in subtropical Mountains: phylogeography, Pleistocene demographic expansion, and evolution of polyphenic mandibles in Taiwanese stag beetle, *Lucanus formosanus*. *Mol Phylogenet Evol* 57: 1149–1161
- Huang XL, Qiao GX, Lei FM (2010a) Use of parsimony analysis to identify areas of endemism of Chinese birds: implications for conservation and biogeography. *Int J Mol Sci* 11: 2097–2108
- Huang ZH, Li NF, Liang W, Zhan YY, Liao XJ, Ruan LZ, Yang ZS (2010b) Phylogeography of Chinese bamboo partridge, *Bambusicola thoracica thoracica* (Aves: Galliformes) in South China: inference from mitochondrial DNA control-region sequences. *Mol Phylogenet Evol* 56: 273–280
- Huang ZG, Zhang WQ, Jiang LM (2005) The characteristics of Quaternary climate fluctuation in the tropics of China. *Geography and Geo-Information Science* 21: 65–70
- Jakobsson M, Rosenberg NA (2007) CLUMPP: A cluster matching and permutation program for dealing with label switching and multimodality in analysis of population structure. *Bioinformatics* 23: 1801–1806
- Jing MD, Yu HT, Bi XX, Lai YC, Jiang W, Huang L (2014) Phylogeography of Chinese house mice (*Mus musculus musculus/castaneus*): distribution, routes of colonization and geographic regions of hybridization. *Mol Ecol* 23: 4387–4405
- Kelly MJ, Edwards RL, Cheng H, Yuan DX, Cai YJ, Zhang ML, et al. (2006) High resolution characterization of the Asian Monsoon between 146,000 and 99,000 years B.P. from Dongge Cave, China and global correlation of events surrounding Termination II. *Palaeogeogr Palaeoclimatol* 236: 20–38
- Knowles LL (2001) Did the Pleistocene glaciations promote divergence? Tests of explicit refugial models in montane grasshoppers. *Mol Ecol* 10: 691–701
- Li BY (1989) On the boundaries of the Hengduan Mountains. *Mountain Research* 7: 15–20
- Li S, Yeung C, Feinstein J, Han L, Manh H, Le MH, et al. (2009) Sailing through the Late Pleistocene: unusual historical demography of an East Asian endemic, the Chinese Hwamei (*Leucodiotron canorum canorum*), during the last glacial period. *Mol Ecol* 18: 622–633
- Liu J, Wang CM, Fu DL, Hu XJ, Xie XM, Liu PF, et al. (2015) Phylogeography of *Nanorana parkeri* (Anura: Ranidae) and multiple refugia on the Tibetan Plateau revealed by mitochondrial and nuclear DNA. *Sci Rep* 5
- Li ZJ, Yu GH, Rao DQ, Yang JX (2012) Phylogeography and demographic history of *Babina pleuraden* (Anura, Ranidae) in southwestern China. *Plos One* 7(3): e34013
- López-López A, Abdul Aziz A, Galián J (2015) Molecular phylogeny and divergence time estimation of *Cosmodela* (Coleoptera: Carabidae: Cicindelinae) tiger beetle species from Southeast Asia. *Zool Scr* 44(2): 437–445
- Maddison WP, McMahon M (2000) Divergence and reticulation among montane populations of a jumping spider (*Habronattus pugillis* Griswold). *Syst Biol* 49: 400–421
- Maekawa K, Kon M, Araya K, Matsumoto T (2001) Phylogeny and biogeography of wood-feeding cockroaches, genus *Salganea* Stål (Blaberidae: Panesthiinae), in southeast Asia based on mitochondrial DNA sequences. *J Mol Evol* 53: 651–659
- Mahmut H, Masuda R, Onuma M, Takahashi M, Nagata J, Suzuki M, Ohtaishi N (2002) Molecular phylogeography of the red deer (*Cervus elaphus*) populations in Xinjiang of China: comparison with other Asian, European, and North American populations. *Zool Sci* 19: 485–495
- Masta SE (2000) Phylogeography of the jumping spider *Habronattus pugillis* (Araneae: Salticidae): recent vicariance of sky island populations? *Evolution* 54: 1699–1711
- McDonald JH, Kreitman M (1991) Adaptive protein evolution at the *Adh* locus in *Drosophila*. *Nature* 351: 652–654

- Papadopoulou A, Anastasiou I, Vogler AP (2010) Revisiting the insect mitochondrial molecular clock: the mid-Aegean trench calibration. *Mol Biol Evol* 27: 1659–1672
- Patriat P, Achache J (1984) India-Eurasia collision chronology has implications for crustal shortening and driving mechanisms of plates. *Nature* 311: 615–621
- Pearson RG, Raxworthy CJ, Nakamura M, Peterson AT (2007) Predicting species distributions from small numbers of occurrence records: a test case using cryptic geckos in Madagascar. *J Biogeogr* 34: 102–117
- Pinot S, Ramstein G, Harrison SP, Prentice IC, Guiot J, Stute M, Joussaume S (1999) Tropical paleoclimates at the Last Glacial Maximum: comparison of Paleoclimate Modeling Intercomparison Project (PMIP) simulations and paleodata. *Clim Dynam* 15: 857–874
- Phillips SJ, Anderson RP, Schapire RE (2006) Maximum entropy modeling of species geographic distributions. *Ecol Model* 190: 231–259
- Posada D (2008) jModelTest: phylogenetic model averaging. *Mol Biol Evol* 25: 1253–1256
- Pritchard JK, Stephens M, Donnelly P (2000) Inference of population structure using multilocus genotype data. *Genetics* 7: 574–578
- Qu Y, Lei F, Zhang R, Lu X (2010) Comparative phylogeography of five avian species: implications for Pleistocene evolutionary history in the Qinghai-Tibetan plateau. *Mol Ecol* 19: 338–351
- Qu YH, Luo X, Zhang RY, Song G, Zou FS, Lei FM (2011) Lineage diversification and historical demography of a montane bird *Garrulax elliotii* - implications for the Pleistocene evolutionary history of the eastern Himalayas. *BMC Evol Biol* 11: 174
- Ronquist F, Huelsenbeck JP (2003) MrBayes 3: Bayesian phylogenetic inference under mixed models. *Bioinformatics* 19: 1572–1574
- Rosenberg NA (2004) Distruct: a program for the graphical display of population structure. *Mol Ecol* 4: 137–138
- Rozas J, Sánchez DBJC, Messeguer PX, Rozas R (2003) DnaSP, DNA polymorphism analyses by the coalescent and other methods. *Bioinformatics* 19: 2496–2497
- Ruddiman WF, Kutzbach JE (1989) Forcing of late Cenozoic northern hemisphere climate by plateau uplift in southern Asia and the American west. *J Geophys Res* 94: 409–427
- Runck A, Cook J (2005) Postglacial expansion of the southern red-backed vole (*Clethrionomys gapperi*) in North America. *Mol Ecol* 14: 1445–1456
- Shi YF, Yao TD (2002) MIS 3b (54–44 ka BP) cold period and glacial advance in middle and low latitudes. *J Glaciology and Geocryology* 24: 1–9
- Simon C, Frati BF, Stewart JB, Beckenbach AT (2006) Incorporating molecular evolution into phylogenetic analysis, and a new compilation of conserved polymerase chain reaction primers for animal mitochondrial DNA. *Annu Rev Ecol Evol S* 37: 545–579
- Slatkin M (1995) A measure of population subdivision based on microsatellite allele frequencies. *Genetics* 139: 457–462
- Swindell SR, Plasterer TN (1997) Seqman. contig assembly. *Method Mol Biol* 70: 75–89
- Swets JA (1988) Measuring the accuracy of diagnostic systems. *Science* 240: 1285–1293
- Tajima F (1989) Statistical method for testing the neutral mutation hypothesis by DNA polymorphism. *Genetics* 123: 585
- Tamura K, Peterson D, Peterson N, Stecher G, Nei M, Kumar S (2011) MEGA5: molecular evolutionary genetics analysis using maximum likelihood, evolutionary distance, and maximum parsimony methods. *Mol Biol Evol* 28: 2731–9
- Wang CS, Ding XL (1998) The new research in progress of Tibet Plateau uplift. *Advances in Earth Science* 13: 526–532
- Wang WJ, McKay BD, Dai CY, Zhao N, Zhang RY, Qu YH, et al. (2013) Glacial expansion and diversification of an East Asian montane bird, the green-backed tit (*Parus monticolus*). *J Biogeogr* 40: 1156–1169
- Wang Y, Chen J, Jiang LY, Qiao GX (2015) Hemipteran mitochondrial genomes: features, structures and implications for phylogeny. *Int J Mol Sci* 16: 12382–12404
- Weisrock DW, Rasoloarison RM, Fiorentino I, Ralison JM, Goodman SM, Kappeler PM, Yoder AD (2010) Delimiting species without nuclear monophyly in Madagascar's mouse lemurs. *Plos One* 5: e9883
- Yeh FC, Yang R, Boyle TBJ, Ye ZH, Mao JX (1997) POPGENE, the user-friendly shareware for population genetic analysis. Molecular biology and biotechnology centre, University of Alberta, Canada, 10
- Ye Z, Zhu GP, Chen PP, Zhang DL, Bu WJ (2014) Molecular data and ecological niche modelling reveal the Pleistocene history of a semi-aquatic bug (*Microvelia douglasi douglasi*) in East Asia. *Mol Ecol* 23: 3080–3096
- Yuan DX, Cheng H, Edwards RL (2004) Timing, duration, and transitions of the Last Interglacial Asian Monsoon. *Science* 304: 575–578
- Zhang DC, Boufford DE, Ree RH, Sun H (2009) The 29°N latitudinal line: an important division in the Hengduan Mountains, a biodiversity hotspot in southwest China. *Nord J Bot* 27: 405–412
- Zhang F, Yu DY, Luo YZ, Ho SYW, Wang BX, Zhu CD (2014) Cryptic diversity, diversification and vicariance in two species complexes of *Tomocerus* (Collembola, Tomoceridae) from China. *Zool Scr* 43: 393–404
- Zhang H, Yan J, Zhang G, Zhou K (2008) Phylogeography and demographic history of Chinese Black-spotted frog populations (*Pelophylax nigromaculata*): evidence for independent refugia expansion and secondary contact. *BMC Evol Biol* 8: 21
- Zhang W, Cui Z, Li Y (2006) Review of the timing and extent of glaciers during the last glacial cycle in the bordering mountains of Tibet and in East Asia. *Quatern Int* 154: 32–43
- Zhao N, Dai CY, Wang WJ, Zhang RY, Qu YH, Song G, et al. (2012) Pleistocene climate changes shaped the divergence and demography of Asian populations of the great tit *Parus major*: evidence from phylogeographic analysis and ecological niche models. *J Avian Biol* 43: 297–310

(Received March 11, 2016 / Accepted July 8, 2016)